

Shear failure induced by waterflooding of a fractured chalk?

H. F. Christensen & K. Hedegaard

GEO, Lyngby, Denmark

C. Høier

DONG A/S, Hørsholm, Denmark

ABSTRACT: Seawater injected into a hydrocarbon bearing reservoir is known to affect the strength and deformation properties, leading to an increase in oil production, but in some cases also to subsidence, compaction or borehole instability. Considering the fractured nature of the reservoirs, it is of major importance to understand the displacement process in conjunction with the fractures. In this study, waterflooding has been carried out at stress states close to shear failure. Local resistance measurements have been used to track the waterfront through the specimen, to indicate fracture flow and to estimate saturation changes. Local strain measurements and resistance data illustrate the displacement process, and whether matrix or fracture plane deformation dominates during waterflooding. The results show that waterflooding does not seem to affect the shear failure condition of the chalk significantly, but it affects the magnitude and nature of the deformations observed in the shear failure phase.

1 INTRODUCTION

1.1 Background

In the chalk fields in the Danish and Norwegian sectors of the North Sea, injection of seawater into oil reservoirs has been used as a very successful secondary recovery mechanism for the last 10-15 years (Andersen 1995). However, the displacement of oil by waterflooding affects the compaction properties of the chalk matrix, which may lead to subsidence of the seabed (Rhett 1990 and Andersen et al. 1992) and borehole instability (Jepsen et al. 2002). Many reservoirs in the North Sea are fractured. The fractured nature of the reservoir may also contribute to the compaction.

Standard rock mechanics tests are most commonly carried out on small-scale specimens with a diameter of 25-50 mm. The specimen size limits the possible amount of fractures, and thus most tests are carried out on non-fractured material. Consequently, an estimate of the fracture-effects has to be made when up-scaling to reservoir scale.

The present laboratory study (part of The Danish Energy Research Program: EFP-2000) focuses on the effect of waterflooding on intact and fractured chalk in relation to the displacement processes (Christensen 2003).

1.2 Laboratory study

It has been observed that for high porosity chalk, waterflooding significantly reduces the pore collapse strength (Christensen 2003). For low porosity chalk a similar reduction is observed, but the pore collapse stress for low porosities is significantly higher than the relevant field stress. This implies that for low porosity chalk, the shear failure strength may be of greater interest than the pore collapse strength.

In this study, three hypotheses regarding the behavior of low porosity chalk, which is waterflooded close to the shear failure condition, were put forward:

Hypothesis 1: Waterflooding re-activates an existing fracture plane.

Hypothesis 2: Waterflooding induces shear failure, if the oil-saturated specimen is waterflooded below the "pre-waterflooding" shear failure line, but above the "post-waterflooding" shear failure line.

Hypothesis 3: Waterflooding reduces the shear failure strength for low porosity chalk so that a "post-waterflooding" shear failure line exists (Fig. 1).

These three hypotheses are tested in the following.

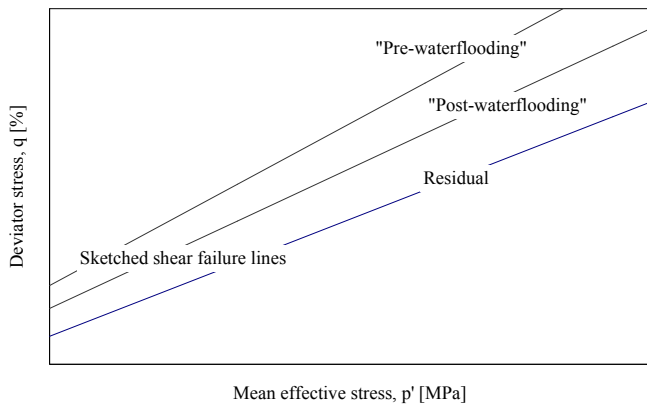


Figure 1. Idealized shear failure lines

2 MATERIAL AND PREPARATION

2.1 Test material and cleaning procedures

All specimens tested were chalk of Maastrichtian age from the Dan Field in the North Sea and they were all estimated to be initially water wet and fully oil-saturated. The specimen characteristics are given in Table 1.

Prior to testing, the specimens were cleaned in methanol and toluene using the cold flush miscible liquids cleaning technique (Springer 1992).

Table 1. Specimen characteristics

Test	Depth ft	Porosity %	Height mm	Diameter mm
7	12608.50	20.1	107.8	54.2
8	12610.75	25.0	78.9	54.1
9	12612.58	24.6	108.1	54.2
17	7615.58	24.9	2076.7	100.0
18	9418.58	22.2	1533.3	100.5
19	9447.83	21.0	2075.5	100.5
22	12606.08	21.8	2076.3	100.3

2.2 Equipment, oil saturation, and waterflooding

The small-scale tests were carried out in a conventional Hoek cell, whereas the medium-scale tests were carried out in a specially developed large scale HOEK cell (SCOT cell), which allows testing of heavily fractured full core specimens ($d = 100$ mm) (Christensen 2003).

The specimens were cold-flush saturated with light laboratory oil (Isopar-L) after installation in the measurement cell.

The specimens were waterflooded with synthetic seawater with a density of 1.024 g/cm^3 . The flooding rates were held constant at $1.5 \text{ cm}^3/\text{h}$ for the small-scale specimens and $11.0 \text{ cm}^3/\text{h}$ for the medium-scale specimens. In some cases, though, it was necessary to use a constant pressure of 700 kPa instead.

Water was injected from the bottom of the specimen in order to avoid air being trapped. Water breakthrough and final water saturation was determined from expelled fluids at the outlet.

Before waterflooding, the specimen was always allowed to be in a creep phase in order to separate the effect of creep and the effect of waterflooding.

2.3 Strain gauges and resistance probes

The small-scale specimens had strain gauges placed at four heights along the specimen and the medium-scale specimens had four strain gauges located at the center of the specimen. Strain gauges measure the deformation locally, which mainly represents the deformation of the chalk matrix.

The medium-scale specimens had probes (stripped wire) placed at eight positions at each side of the specimen (Fig. 2). The probes measure the resistance through a lentil-shaped cross-section of the specimen. In order to achieve good contact to the matrix, the probes were placed in undersized holes drilled in the specimen.

The present set-up is based on resistance measurements carried out by Høier (2002). The simple set-up makes it possible to measure the resistance during extensive compaction at axial and radial stresses corresponding to reservoir conditions, because the probes and wires are able to follow the movement of the specimen.

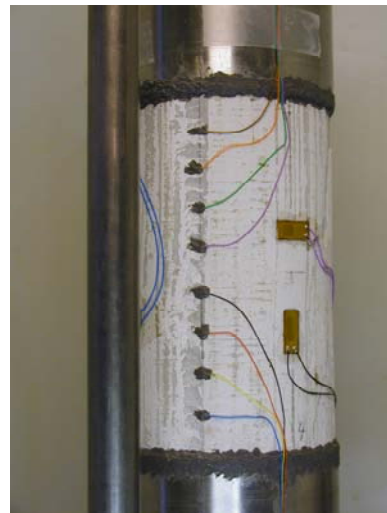


Figure 2. Resistance probes and strain gauges (Medium-scale specimen)

3 FRACTURE OR MATRIX DOMINATED DEFORMATION

Distinction between deformation of the chalk matrix and movement in the fracture plane may be done by comparison of the local strain rate of the matrix (measured by strain gauges) and the overall strain rate of the specimen (measured by external deformation measurements).

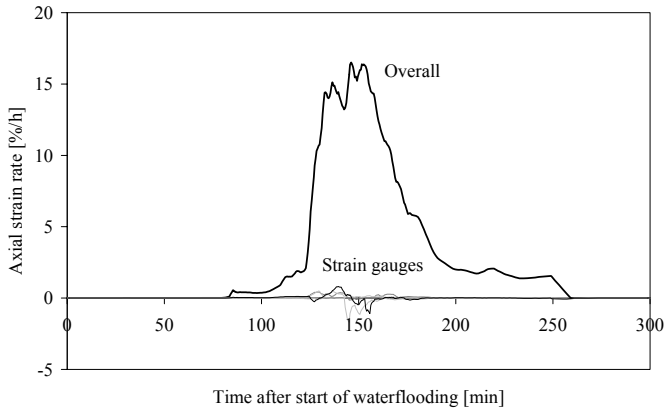


Figure 3. Movement in the fracture plane

In case of movement in the fracture plane, the chalk matrix deforms at a very low strain rate, whereas the whole specimen deforms at a considerably higher strain rate (Fig. 3).

In case of elastic deformation of the matrix, both the matrix and the specimen deforms at a very low strain rate (Fig. 4). The same behavior will show for plastic deformation (e.g. compaction above the pore collapse stress level), but the strain rates will be considerably higher.

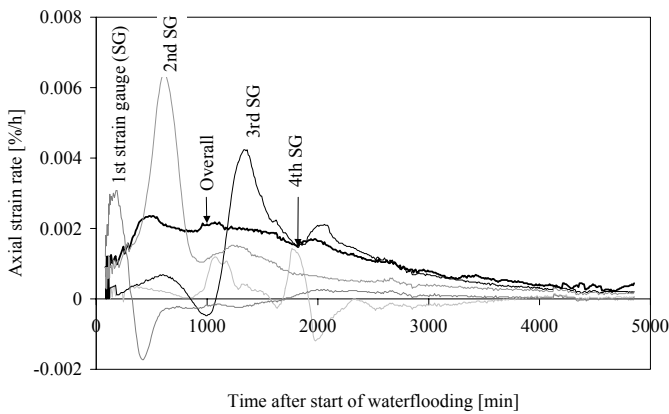


Figure 4. Elastic deformation of the matrix

4 FRACTURE OR MATRIX DOMINATED FLOW

Distinction between fracture and matrix dominated flow may be done by resistance measurements in relation to the amount of injected water.

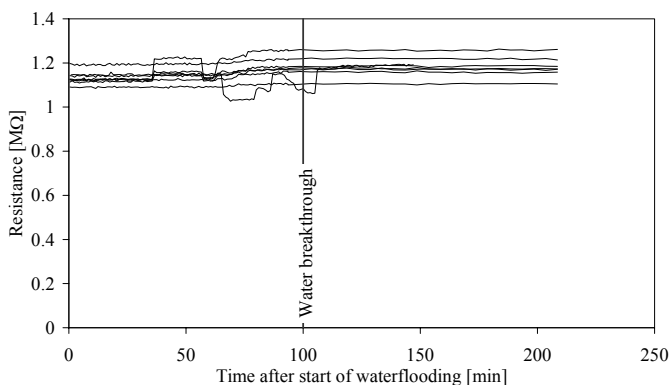


Figure 5. Response from probes (Ideal fracture flow)

In case of ideal fracture flow, the resistance probes, which sit in the matrix, do not detect the water that moves past. Therefore, the probes measure a constant high resistance, even though water breakthrough is observed at the outlet (Fig. 5).

In case of matrix flow, the probes measure a high resistance until they detect the water. Then they show a distinct jump from high to low resistance (Fig. 6).

The nature of the matrix flow may be determined by plotting the movement of the water front, detected by resistance probes, through the specimen. The response times were read at resistances of 0.2 MΩ. The plots are shown later in Figures 11 and 12.

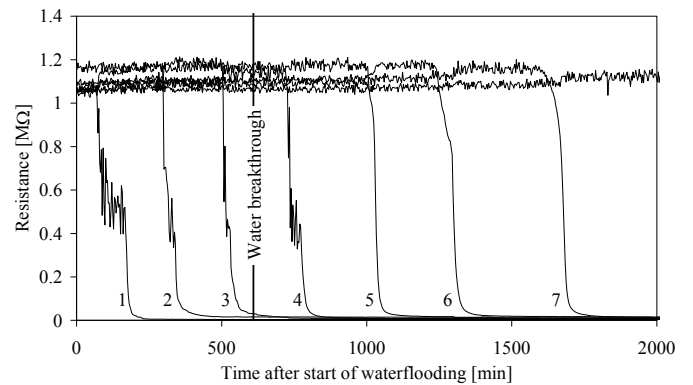


Figure 6. Response from probes (Example of matrix flow)

5 STRESS PATHS

The stress paths are shown in the (p'-q)-plots (Fig. 7 and 8). The mean effective stress $p' = (\sigma_1 + 2\sigma_3)/3$ and the deviator stress $q = \sigma_1 - \sigma_3$, where σ_1 is the axial stress and σ_3 is the radial stress. All the specimens follow a uniaxial compression path towards shear failure. A general loading rate of 0.1 %/h was applied.

The shear failure trends in the figures are calculated on the basis of shear failure data for Maastrichtian chalk in a neighboring oil field.

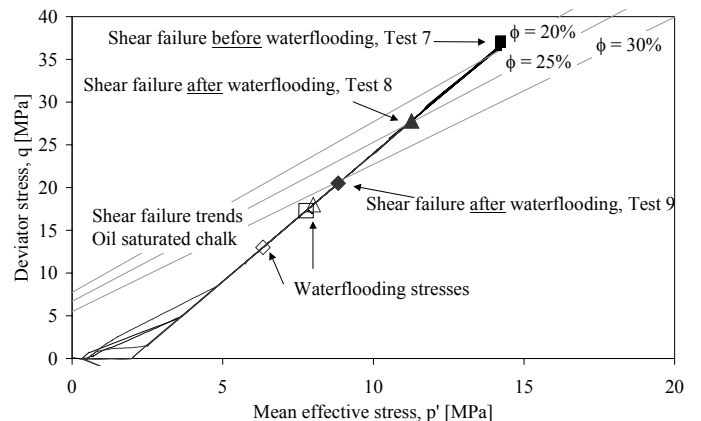


Figure 7. (p'-q)-plot (Small scale specimens)

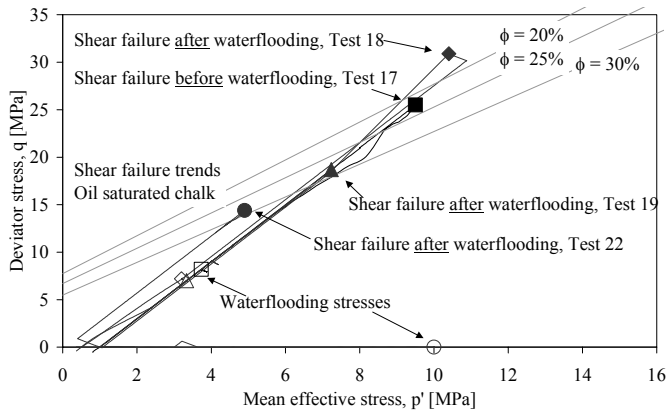


Figure 8. (p'-q)-plot (Medium scale specimens)

6 TEST RESULTS

In the following, the three hypotheses are tried answered.

The residual stress state has been chosen as a lower boundary for the waterflooding stress as it is the stress state where fractured chalk resides. All waterflooding tests were carried out at a stress level at or slightly above the residual stress state of the chalk.

6.1 Hypothesis 1: Waterflooding re-activates an existing fracture plane

The specimens (Tests 7 and 17) were first loaded to shear failure in order to create a fracture plane. One specimen was waterflooded immediately after shear failure (Test 7) and one was allowed to stabilize at the residual stress state before waterflooding (Test 17). In both cases the specimens experienced extensive deformation after being waterflooded for 250 and 71 min, respectively (Fig. 9). By plotting the local and external strain rates against time, it is evident that movement in the fracture plane causes the deformation.

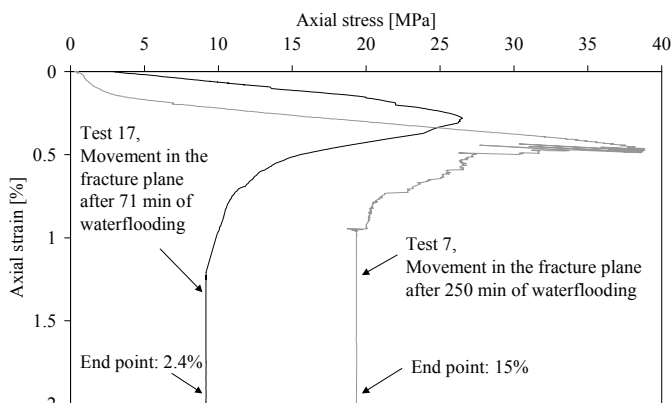


Figure 9. Stress-strain

The resistance measurements further support this observation. During waterflooding, the resistance probes measured a high resistance as in Figure 5, which indicate very low water saturation. However, knowing that water was injected into the specimen and oil was expelled, it is reasonable to believe that the water ran through the fracture instead of the matrix. Furthermore, the specimen capsized, before water breakthrough was observed, which indicate that water smeared the fracture and caused the shear plane to be re-activated.

6.2 Hypothesis 2: Waterflooding induces shear failure

The specimens (Tests 8, 9, 18, and 22) were loaded to or above a stress state comparable to the residual stress state. The still intact, non-fractured chalk specimens were then waterflooded for 167, 188, 139, and 36 hours, respectively. The waterflooding only resulted in a minor deformation (Fig. 10). By plotting the strain rates against time, it becomes evident that the deformation is caused by elastic deformation of the chalk matrix. Shear failure was not induced by waterflooding at this stress state.

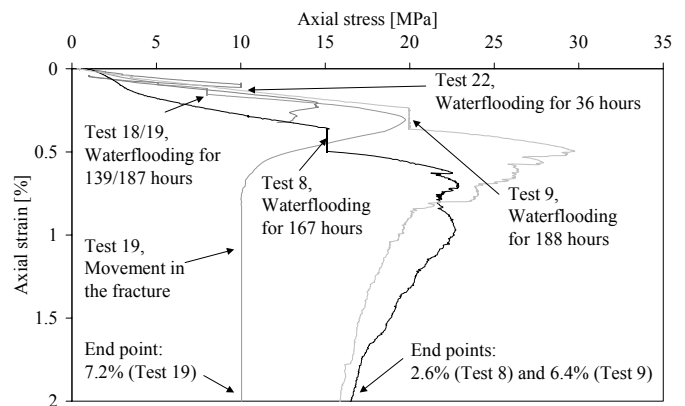


Figure 10. Stress-strain

Figure 11 shows the position of the waterfront, based on water injected through Test 22. It indicates a piston-like movement of water through the matrix.

The position of the waterfront based on the resistance measurements show a similar trend.

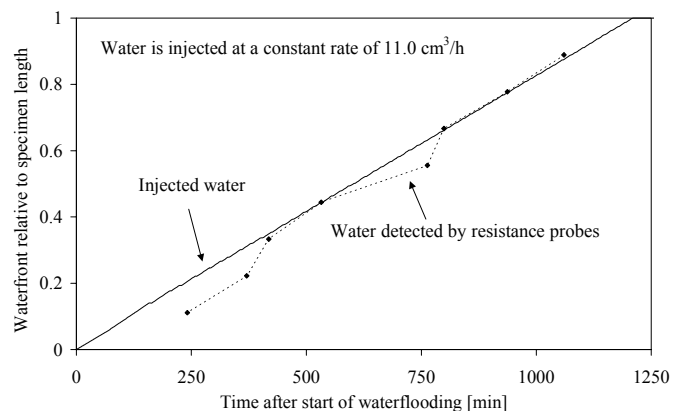


Figure 11. Movement of waterfront (Test 22)

Figure 12 shows the movement of the waterfront through Test 18 as a piston-like displacement. The decreasing slope is caused by a decreasing flow rate due to a constant injection rate. The resistance probe measurements show a similar trend. However, this line has a different slope as if the probes see the water later than expected from the injected water and expelled fluids. The reason may be that the water moves through the specimen with a tilted or diffuse waterfront.

Water breakthrough happened according to the resistance probes, when only three probes had detected water (Fig. 14), which further indicates a tilted/diffuse waterfront.

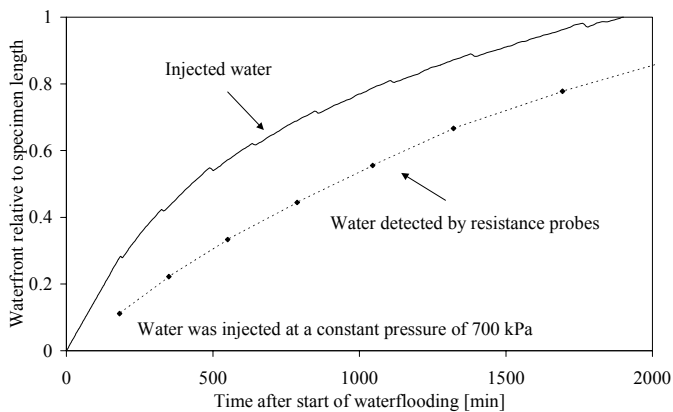


Figure 12. Movement of waterfront (Test 18)

6.3 Hypothesis 3: Waterflooding reduces the shear failure strength

The shear failure strength of the oil-saturated specimens (Tests 7 and 17) is shown in Figure 7 and 8. Tests 8, 9, 18, and 22 were all waterflooded at or slightly above a stress state similar to residual stress state, and afterwards loaded to shear failure. They fail in shear with water saturations of $S_w = 0.42$, 0.92, 0.48, and 0.58, respectively. When comparing the two oil-saturated specimens to the "pre-waterflooding" trendlines it is seen that they both fail very close to their trendlines. In contrast, the partly water saturated specimens (except Test 18) fail at a slightly lower stress, corresponding to a softer or more porous chalk. However, the water-induced reduction is small compared to the difference between the "post-waterflooding" and the residual shear failure lines.

6.3.1 Delayed activation of fracture plane

Test 19 was carried out as Tests 8, 9, 18, and 22. After waterflooding it was loaded to shear failure, allowed to stabilize at residual stress and left to creep. After 294 min, large deformation of the specimen occurred (Fig 10). The strain rates indicate that movement in the fracture plane causes the deformation.

The fracture was activated after a time delay, which is comparable to the time necessary for water-induced re-activation of an existing fracture (Tests 7 and 17). The reason why the specimen does not deform immediately when the fracture is generated may be that time is needed for redistribution of the water along the created fracture plane. The average water saturation of the specimen was $S_w = 0.45$ when the fracture plane was generated.

So, even though waterflooding does not reduce the shear failure strength, it may affect the magnitude of the deformation at the residual stress state.

7 ESTIMATED WATER SATURATIONS

The resistance measurements may also be correlated to water saturations by using an implicit method developed by Olsen (1990). The method aims at minimizing the difference between the injected amount of water and the water volume measured by the probes (as different levels of resistance). It may only be used when a homogeneously distributed porosity and thereby homogeneous saturation exist along the length of the specimen and only until the final water saturation is reached.

Due to the interdependence of the resistances, malfunction of probes has to be taken into account when interpretation of the saturation plot is made. However, by adjusting the supposedly wrong water saturation(s) from the malfunctioning probes to the correct final saturation, the rest of the saturation(s) will also stabilize at this saturation.

Examples of saturation calculations without adjustments are shown in Figures 13 and 14.

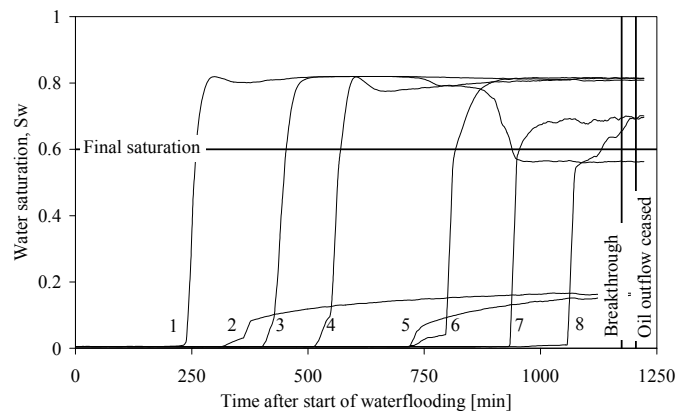


Figure 13. Water saturations (Test 22)

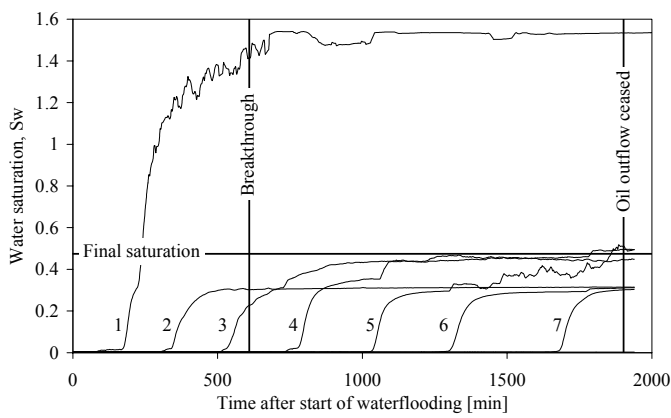


Figure 14. Water saturations (Test 18)

8 CONCLUSION

It should be noted that the following conclusions are based on testing of low porosity chalk in the elastic regime. The conclusions may be different for high porosity chalk at higher stress levels

Hypothesis 1: Waterflooding re-activates an existing fracture plane

The ability to withstand deformations along an existing fracture plane is greatly reduced when waterflooding has been carried out.

Waterflooding of already fractured chalk results in an immediate large deformation of the specimen. Probably, the water prefers to run through the fracture, which becomes water saturated. The water smears the fracture and makes the chalk deform along the fracture plane.

Waterflooding of intact, non-fractured chalk, which afterwards is fractured, may also result in movement along the fracture plane. Only, in this case there seems to be a delay of the deformations. A possible explanation is that the water smears the fracture, but because the fracture is only partly water saturated, it takes a while before the specimen starts to deform.

Hypothesis 2: Waterflooding induces shear failure

Non-fractured chalk was waterflooded at a stress level below the "post-waterflooding" shear failure line, but above the residual shear failure line. No indication of generation of a fracture plane is seen.

Hypothesis 3: Waterflooding reduces the shear failure strength

Waterflooding seems to cause a slight reduction of the shear failure strength, but the reduction is small compared to the difference between the "post-waterflooding" shear failure line and the residual shear failure line. However, the waterflooding affects the magnitude of the observed deformation.

9 IMPROVEMENTS OF SET-UP

Comparison of strain rate measured by strain gauges and external deformation measurements gives a good indication of the type of deformation; whether dominated by matrix deformation or movement along a fracture plane.

This method may be further improved by increasing the number of strain gauges on the specimen or simply by placing the strain gauges at the same levels as the resistance probes.

Resistance measurements give a good indication of whether the waterfront moves through matrix or fractures.

Furthermore, it is possible to calculate water saturations from resistance measurements when compared with the water breakthrough and final water saturation. Due to interdependence of the resistances, one malfunctioning probe may lead to false saturations. A possible way to avoid this is to saturate the specimens to a low initial water saturation of e.g. $S_w = 0.05$ in order to get a well defined reference level.

Furthermore, the set-up may easily be extended with more probes and/or by cross-measurements between selected probes.

10 ACKNOWLEDGEMENTS

The EFP-2000 is funded by The Danish Energy Authority and co-funded by BP Norway and Mærsk Oil and Gas AS.

The work was carried out in close cooperation with GEUS core laboratory that supplied special core analysis as well as know-how, equipment and software for the resistance measurements.

DONG A/S is thanked for giving C. Høier the opportunity to finish the work on interpretation of resistance measurements that he started at GEUS.

REFERENCES

- Andersen, M. A. 1995. Petroleum Research in North Sea Chalk. Joint Chalk Research, Phase IV.
- Andersen, M. A., Foged, N. & Pedersen, H. F. 1992. The Link between Waterflood-induced Compaction and Rate-Sensitive behaviour in a weak, North Sea chalk. 4th North Sea Chalk Symposium, Deauville.
- Christensen, H. F. 1996. Rock Mechanics and Water Injection - Waterflooding of Chalk. Joint Chalk Research, Phase IV
- Christensen, H. F. 2003. EFP-2000 Displacement and deformation processes in fractured reservoir chalk, compilation report. EFP-2000.
- Høier, C. 2002. EFP-2000: Displacement and deformation processes in fractured reservoir chalk - Determination of a moving water front in core samples using resistance logging: Hardware and software user manual. EFP-2000.
- Jepsen, J.-E. 2002. Plane Finite Element Model - Two-Dimensional Geomechanics Finite Element Simulation of

Reservoir Deformation and implications for Well Failure in the Valdemar Field. EFP-97.

Olsen, N. K. 1990. Two-Phase Flow in Fractured Porous Media. P.hD thesis at Laboratory for Energetics, Technical University of Denmark,

Rhett, D. W. 1990. Long Term Effects of Water Injection on Strain in North Sea Chalks. 3rd North Sea Chalk Symposium, Copenhagen.

Springer, N. 1992. Preparation of Chalk for Petrophysical Experiments. 4th North Sea Chalk Symposium, Deauville.